# Steady Laminar Natural Convection Heat Transfer inside Air-Filled Horizontal Triangular Enclosure Containing Three Cylindrical Rods

Falah Assi Abood Muneer A. Ismael
Mechanical Engineering Department - College of Engineering
University of Basrah

Abstract:

The natural convection heat transfer from horizontal isothermal three cylindrical rods inside equilateral triangular enclosure has been studied numerically. The enclosure is filled with air, and the heated rods are located at equal distances (E) from triangle center. A finite element software package (FLEXPDE) is used in the present study to solve the set of non-linear equations governing the process. Solutions are obtained for aspect ratio D/H=1/6 and range of distance E=0.2-0.6 and Rayleigh (Ra) number changes from $10^3$ to $10^6$. The effect of Ra and E were examined. Results are presented by streamlines, isotherms and Nusselt number and it indicates that the Nusselt number is significantly increase with increasing both Ra and E. A comparison of the Nusselt number was made with that obtained by [7], and showed substantial improvement to about 65% in some cases.

## إنتقال الحراره بالحمل الحر الطباقي المستقر داخل وعاء مثلث أفقي مملوء بالهواء و يحتوي على ثلاثة قضبان أسطوانية

فلاح عاصي عبود منير عبد الجليل اسماعيل

قسم الهندسة الميكانيكية– كلية الهندسة– جامعة البصره

**الخلاصة:**

تم في هذا البحث دراسة عددية لعملية إنتقال حرارة بالحمل الحر من ثلاث قضبان اسطوانية مسخنة ذات درجة حرارة ثابتة داخل وعاء (enclosure) مثلث متساوي الاضلاع. الوعاء مملوء بالهواء والقضبان المسخنة موضوعة على مسافات متساوية (E) من مركز الوعاء المثلث. تم استعمال حقيبة برمجية تعمل بطريقة العناصر المحددة ( FLEXPDE) لحل منظومة المعادلات اللاخطية الحاكمة لعملية انتقال الحرارة هذه. النتائج المستحصلة لنسبة ثابتة من قطر القظيب الى ارتفاع المثلث (aspect ratio) (D/H=1/6) و قيم E تتراوح من 0.2 إلى 0.6 و رقم رايلي (Rayleigh) Ra من $10^3$ إلى $10^6$ حيث تمت دراسة تأثير كل من Ra و E . بينت النتائج التي مُثلت بواسطة خطوط الجريان (streamlines) و خطوط التحارر (isotherms) ورقم نسلت (Nusselt number) , بينت بأن رقم نسلت يزداد بازدياد كل من E و Ra . قورنت النتائج المستحصلة مع ما منشور في المصدر [7] وأظهرت تحسن كبير في رقم نسلت يصل في بعض الحالات إلى 65.0% .

## 1. Introduction

Over the past decades, internal (in enclosure) and external natural convection heat transfer has important engineering applications. Several studies have been achieved in the problem of laminar flow forced convection in ducts (enclosures) of various cross-sections because of its applicability in various fields such as compact heat exchangers, air conditioners, nuclear reactors, solar collectors, solar stills, electronic cooling etc. Among these various cross-section ducts is the triangular cross-sectional duct which is preferred in most situations due to its simplicity in manufacturing and placing. The first study published in this field is by Flack *et al* [1,2] where they focused in measurement of natural convection heat transfer in isosceles triangular enclosure with two isothermal sides and an insulating bottom. Their important conclusion is that the local Nusselt numbers are slightly depend on the angle (and hence on the triangle height) between the isosceles sides. Besides to the triangular geometry, further irregular geometries cross-sections like rhombic, sinusoidal and other irregular cross-sections were studied numerically by Ibrahim and Mazhar [3]. Asan and Namli [4] presented the results of a numerical investigation of laminar natural convection in triangular cross-section. The effect of Rayleigh number and height/base ratio on the flow structure and heat transfer has been studied. A similar study with approximately the same conclusion is done by Kent [5]. In fact, thermal performance of a duct is reduced when the circular cross-sectional geometry is not used. However it is able to enhance thermal performance by inserting some bodies inside say triangular enclosure i.e. introducing an annular flow. Hence, and due to the recent development in both numerical and manufacturing techniques, the attention of researchers is directed into flow through new geometries of concentric non-circular ducts. Roa *et al* [6] studied the problem of laminar flow heat transfer in channels of annular cross-sections formed by concentric equilateral triangles. They proved that in certain case the thermal performance of their geometry is better than the concentric circular annular channel for constant wall temperature boundary condition. More recently, numerical extensive data of a laminar convective heat transfer around horizontal cylinder within its concentric air-filled equilateral triangular enclosure have been performed by Xu Xu et al [7]. Those authors analyzed the effect of Rayleigh numbers, aspect ratio, the shape of inner cylinder and the inclination angle of enclosure on the heat transfer process.

A survey of literature reveals that multi-inner cylinder inside air-filled triangular enclosure has not been investigated. This is the motivation of the present study where three circular cylinders inside an equilateral triangular enclosure is to be used. The effect of Rayleigh number and cylinders position on the flow and thermal fields for constant aspect ratio are studied in details. The flow is considered as laminar rather than turbulent because the laminar flow was proven to be more efficient especially in heat exchanger application [6]. Only one cross section, circular, of the inner cylinders was studied and the enclosure rests on its bottom base without any inclinations angle as these two factors have insignificant effect on the performance of the enclosure [7].

## 2. Governing equations

Consider laminar natural convection of (Newtonian fluid) in an equilateral triangular enclosure containing three circular rods of equal radii located at equal distances E from the triangle center. The temperature of rods walls ($T_i$) is higher than that of the triangle wall ($T_o$) and both are uniform. The lengths of both enclosure and rods are assumed to be extremely large, therefore considering only the variations over the cross-section will not affect the simulation of the practical process. The interest domain is shown in Fig.1. The origin of the cartesian coordinates (x,y) is positioned at the triangle center. The aspect ratio (rod diameter/triangle height) is fixed in this study to be D/H=1/6. The fluid is assumed to have constant physical properties but obeys the Bussinesq approximation according to which the compressibility effect every where is neglected except for Buoyancy force term. Viscous dissipation and heat generation are absent. Hence, the two-dimensional, incompressible, steady state dimensionless governing equations using conservation of mass, momentum and energy can be written as:

$$\frac{\partial U}{\partial X}+\frac{\partial V}{\partial Y}=0 \tag{1}$$

$$U\frac{\partial U}{\partial X}+V\frac{\partial V}{\partial Y}=-\frac{\partial P}{\partial X}+\frac{\partial^2 U}{\partial X^2}+\frac{\partial^2 U}{\partial Y^2} \tag{2}$$

$$U\frac{\partial V}{\partial X}+V\frac{\partial V}{\partial Y}=-\frac{\partial P}{\partial Y}+\frac{\partial^2 V}{\partial X^2}+\frac{\partial^2 V}{\partial Y^2}+\left(\frac{Ra}{\Pr}\right)\theta \tag{3}$$

$$U\frac{\partial \theta}{\partial X}+V\frac{\partial \theta}{\partial Y}=\frac{1}{\Pr}\left(\frac{\partial^2 \theta}{\partial X^2}+\frac{\partial^2 \theta}{\partial Y^2}\right) \tag{4}$$

Non-dimensional parameters are defined as follows:

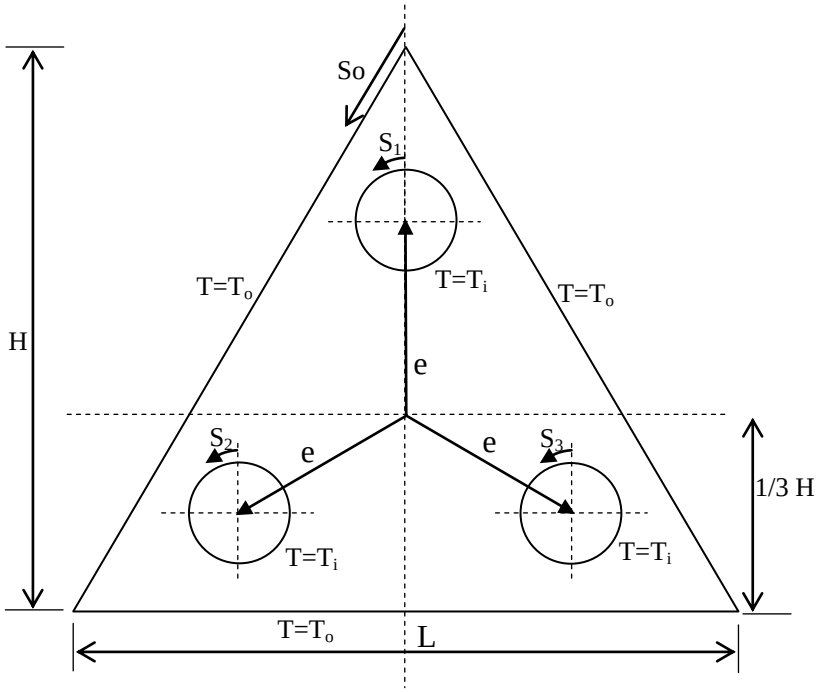


Fig.1 Schematic diagram of the physical domain.

$$X=\frac{x}{H},\ Y=\frac{y}{H},\ E=\frac{e}{\frac{2}{3}H},\ U=\frac{uH}{\upsilon},$$

$$V=\frac{vH}{\upsilon},\ \theta=\frac{T-T_o}{T_i-T_o},\ and\ P=\frac{(p+\rho gy)H^2}{\rho v^2}$$

Rayleigh number $Ra=\frac{g\beta(T_i-T_o)H^3}{\upsilon\alpha}$, and

Prandtl $\Pr=\frac{\upsilon}{\alpha}$

## 3. Numerical solution

It is well known in the numerical solution field that the set of equations (1-4) may be highly oscillatory or even sometimes undetermined because of the inclusion of the pressure term in the momentum equations. In the present study, a finite element software package (Flexpde) [8] is used in the solution of the nonlinear system of equations. In finite element method there is a derived approach with purpose of stabilizing pressure oscillations and allowing standard grids and elements. This approach enforces the continuity equation and the pressure to give the following, what called, penalty approach, [9]

$$\nabla^2 P=\lambda\left(\frac{\partial U}{\partial X}+\frac{\partial V}{\partial Y}\right) \qquad (5)$$

where $\lambda$ is a parameter that should be chosen either from physical knowledge or by other means [9]. A most convenient value for λ was attained in this study to be $1x10^{11}\mu/H^2$.

Hence, the continuity equation (1) is excluded from solution system and replaced by equation (5). The continuity equation is used to check the error of the solution throughout the grids of domain.

The appropriate boundary conditions are as follows:

1- Isothermal surfaces i.e. θ=1 on the rods walls and θ=0 on the triangle walls.

2-No-slip velocity boundary condition, U=V=0 on all solid walls.

3- Pressure gradient normal to all surfaces is zero, $\frac{\partial P}{\partial \boldsymbol{n}} = 0$ where $\boldsymbol{n}$ is a normal unit vector.

### 3.1 Software validation

To check the accuracy of the present numerical method and enhance the reliability of the obtained results, five grid densities were examined. Prandtle number has been slightly effected and is assumed to be constant throughout the present study, on the other hand the grid dependency were checked with Rayleigh number. Figure 2 shows the distribution of the average Nusselt number of the triangle walls as a function of relative error, where in this package, the grid sizes can be controlled by imposing a relative error and the times of adaptively mesh refinement, which is fixed here at three times adaptive refinement. It can be seen that approximately when $Ra<10^6$, the results are independent on grid sizes, but when $Ra=10^6$, the values of average Nusselt number are the same when the relative error is set lesser than $10^{-4}$. Therefore an accuracy of $10^{-5}$ was chosen in this study as a compromise between the results accuracy and the time consumed in each run. The maximum time in some cases takes about 2700 seconds. The girded domain is shown in Fig. 3a. The distribution of the values of ($\partial U/\partial X + \partial V/\partial Y$) over the domain is presented in Fig.3b. It is clear that the continuity equation is exactly validated, where it as mentioned in section 3, does not contribute in solving the governing equations.

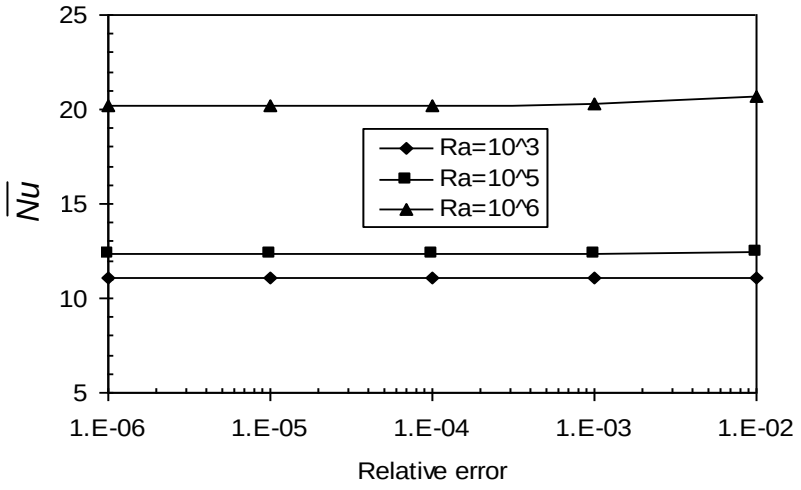


Fig.2 Average Nusselt number dependency on the imposed accuracy, D/H =1/6, E=0.3

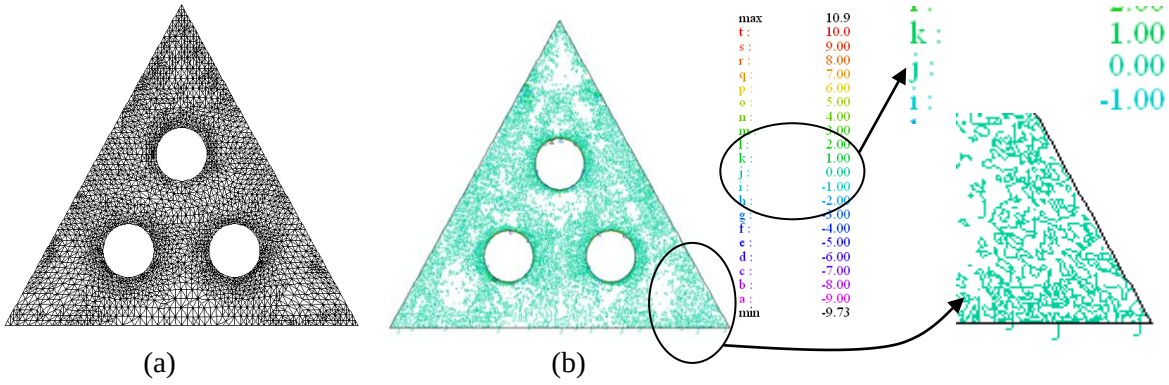


(a) (b)

Fig. 3. For $10^{-5}$ accuracy and E=0.3, (a) grid distribution over the domain (b) validation of continuity equation

### 3.2 Validation of numerical results

Most researchers work focused on the study of natural convection in annuli between either concentric or eccentric circular cylinders and between a square outer cylinder and a circular inner cylinder. Only a few publications were involved in an annulus between a triangular outer enclosure and a circular inner cylinder. In the work of Xu Xu *et al* [7], the circular inner heated cylinder was concentrically located inside a triangular cylinder, the governing equations were iteratively solved with the convergence criteria of $10^{-4}$ for each variable. As shown in Fig.4, the computed local Nusselt number distribution (after adapting the present physical model to be of one concentrated circular inner heated cylinder) along the outer wall predicted in the present study was compared with the values reported by [7]. In general, very good agreement between the two results was obtained. Finally the comparison of the overall heat transfer rate was also undertaken. The values of average Nusselt number along the outer wall of Ref. [7] for $Ra=10^3$ is 15.49 and the computed value here is 15.544 with a deviation less than 0.413 %. The agreement between the two results is satisfactory. Knowing that this computation was achieved after adapting the present code to be of one concentric rod of aspect ratio of 1/2.

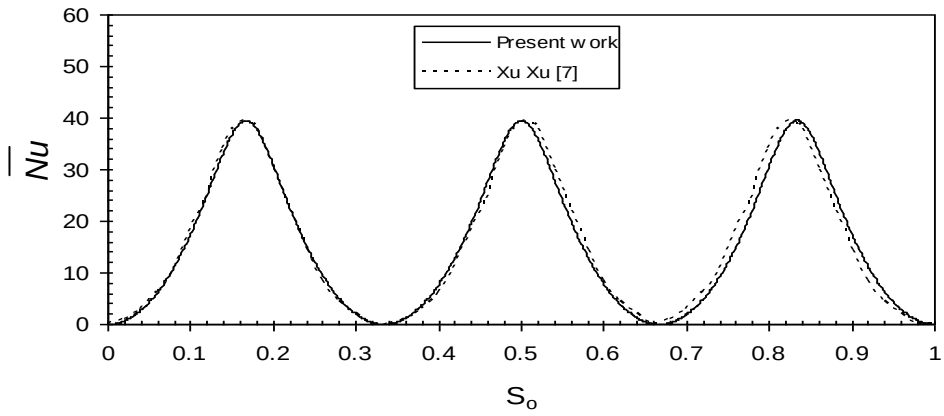


Fig.4 Comparison of local Nusselt number on the triangle walls with [7], for single concentric rod, D/H=1/2, $Ra=10^3$

## 4. Results and discussions

In the present study, the effect of the Rayleigh number ($10^3$, $10^5$ and $10^6$) and the location of the inner rods (E=0.2-0.6) were systematically investigated. The Prandtle number is set to be 0.71. The equations (2-5) are solved using a finite element software package (FLEXPDE). Nusselt numbers are defined in the same way as shown in the work of Mukallad and Acharya [10].

### 4.1 Analysis of flow fields

Analysis of the flow is displayed by mean of stream function $\psi$ obtained from velocity components $U$ and $V$. The relationships between stream function $\psi$ and velocity components for two dimensional flows are: $U = \frac{\partial \psi}{\partial Y}$, $V = -\frac{\partial \psi}{\partial X}$ which yield a single equation:

$$\frac{\partial^2 \psi}{\partial X^2} + \frac{\partial^2 \psi}{\partial Y^2} = \frac{\partial U}{\partial Y} - \frac{\partial V}{\partial X} \qquad (6)$$

where $\psi$ is zero on all surfaces The streamlines are shown in Fig.5, in which the subfigures were arranged going down with increasing Rayleigh number and going from left to right with decreasing the distance between rod centers and triangle center (E). Due to the buoyant effects caused by the temperature difference between the inner and outer walls, recirculation vortices are formed which are clearly demonstrated by the closed stream lines. It is shown in Fig.5, that at low Rayleigh number ($Ra=10^3$) the flow fields are nearly symmetric for each E. This is attributed to the weak convection current compared with conduction inside the enclosure and this is clearly appearing from the values of the stream lines shown in Fig.5. For E=0.6 the flow field show that the four centers of four symmetric eddies among inner heated cylinder is closer. This is because the large space available for circulation to occur when E increases. As E is reduced, the streamlines become denser around the inner heated walls and are separated into two vortices. It is also noticed that at lower E=0.2 the flow pattern recovers nearly symmetric feature since the gap between the inner heated cylinder is extremely narrowed. For higher Rayleigh numbers $Ra=10^6$ and E=0.6, the streamlines become denser in the region among the rods, as shown in Fig.5c, and two large eddies are found above the bottom two cylinders. With decreasing E this eddies become more distorted and are thus separated to form the new vortices in the left and right side of the geometry. Two additional eddies are formed on top of the upper cylinder, the additional eddies disappear and become weak. This is an interpretation to that the further increase of Rayliegh number increases the circulation strength inside the enclosure. Using the above definition of the stream function, the positive sign of $\psi$ denotes anti-clockwise circulation and the clockwise circulation is represented by the negative sign of $\psi$.

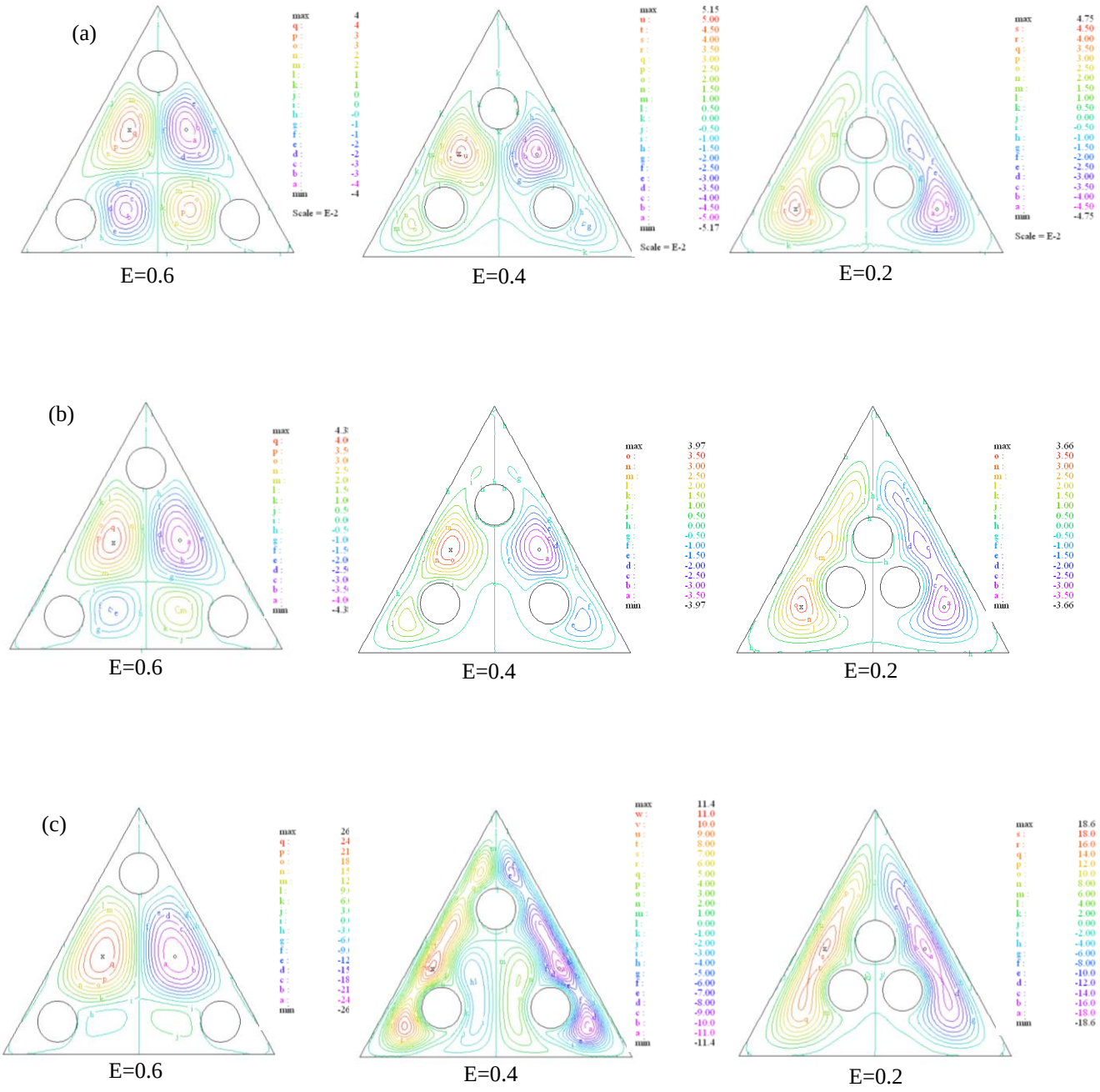


Fig.5 Streamlines for (a) Ra=$10^3$, (b) Ra=$10^5$, (c) Ra=$10^6$ for different values of E

## 4.2 Analysis of thermal fields

The thermal fields are presented in the form of isotherms in Fig.6 with the same arrangement of Fig.5. At lower Rayleigh numbers, the isotherms are similar to those of the case of pure conduction since the intensity of the buoyancy-driven convection is very weak and the thermal field is thus nearly unaffected. Increased discrepancies against the pure conduction cases can be found as the Rayleigh number goes higher. The isotherms become denser and more concentrated to the upper region. At the highest Ra and E, separation of the thermal

boundary layer is clearly observed. At lower distance E, the isotherms along the top of the upper cylinder separate away from its upper zone and form a thermal plume impinging vertically to the apex corner of the enclosure. The formation of the plumes becomes more intensive for $Ra=10^6$ and E=0.2.

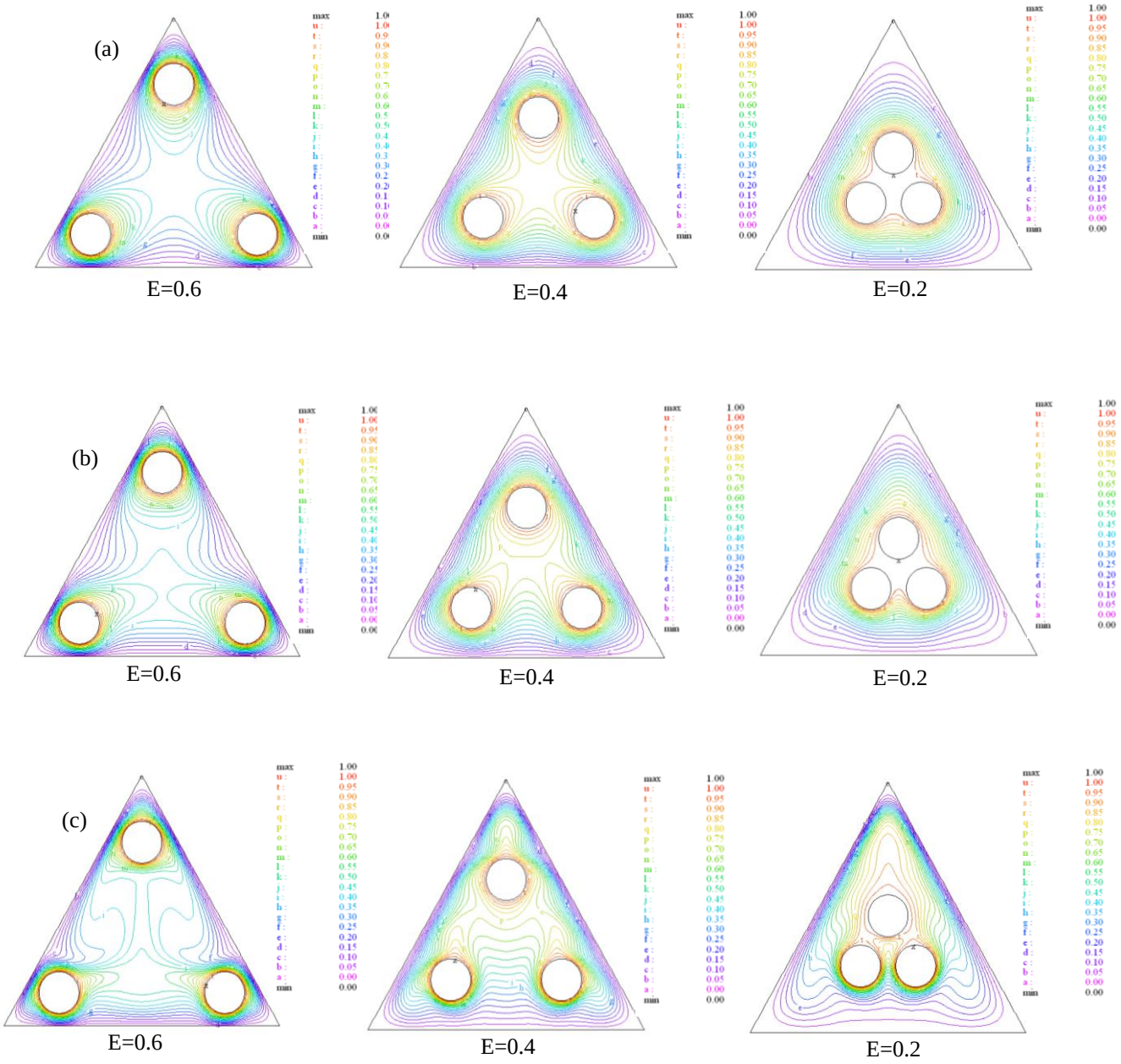


Fig.6 Isotherms for (a) $Ra=10^3$, (b) $Ra=10^5$, (c) $Ra=10^6$ for different values of E

### 4.3 Nusselt Number

The local heat transfer coefficient *h* along each inner rod wall and the outer wall are expressed as:

$$h = -k\frac{\partial T}{\partial \boldsymbol{n}} \qquad (7)$$

where *k* is the thermal conductivity. The local Nusselt numbers for both outer surfaces and each inner heated surface are determined by:

$$Nu_o = \frac{h_o L_o}{k} \quad , \quad Nu_i = \frac{h_i L_i}{k} \qquad (8)$$

where $L_i=\pi D$ and $L_o = 2\sqrt{3H}$ are the perimeters of the cross sections of the inner rod and the outer triangle respectively [7].

Variation of the local Nusselt number around the upper cylinder is plotted in Fig.7a where the subscripts of the local Nusselt number and the local coordinated are dropped. When the Rayleigh number is low, the curves show two peaks with nearly equal altitude at the left and right sides of cylinder exactly at $S_1=0.125$ and $S_1=0.825$ which are closer to the triangle walls. These peaks of Nusselt number appear because the temperature difference between the circular surfaces portions of $S_1$ and the triangular enclosure is minimum here. In contrary, the local heat transfer rates at the upper region of the upper cylinder (around $S_1=0$ or $S_1=1$) also at left and right sides ($S_1=0.3$, $S_1=0.7$) become lower with increasing Rayleigh due to the previous mentioned thermal layer separation that reduces the local heat transfer between air and wall. At the bottom region of the upper cylinder ($S_1=0.5$) the local Nusselt number is increased with increasing Rayleigh number where the effect of convection isincreased. On the other hand for low E (0.2), curves show also two peaks for $Ra=10^3$ and $Ra=10^5$ but it differ from that of E=0.6 is that the value of Nusselt number at $S_1=0.5$ is zero. This means that the conduction is completely dominated here. While at $Ra=10^6$, one peak appears at $S_1=0.5$ which indicate to the large effect of convection here. Fig 7b depicted the variation of local Nusselt number around the surface of bottom cylinder which is located at the left side of the enclosure. More peaks and troughs are observed, which mostly appear around the cylinder surface. With decreased E (=0.2), the local heat transfer rates at $0.2<S_2<0.8$ become much greater as the Rayleigh number is increased, which in turn increase the convection effect, resulting in bell-shaped curves that can be seen from Fig.7b. The distribution of the local Nusselt number around the right bottom cylinder surface ($S_3$) is exactly same as that of the left one but with opposite direction from left to right hence, this distribution is not displayed.

The local peripheral Nusselt number of the outer triangular enclosure exhibits apparent

piece wise feature over three side walls. Fig.7c shows the variation of $Nu_o$ for E=0.6. The curves for each Rayleigh number show two equal peaks for each side of outer surface. The reason of this behavior could be drawn from the isotherms (Fig.6 a-c) at E=0.6, where in each enclosure side there are two positions adjacent to two inner heated cylinders. In these positions the temperature difference is low, hence Nussuelt becomes large. The altitudes at left and right side walls are higher than that at bottom wall for $Ra=10^6$ because of the effect of convection. When E=0.2, the curve for lower Ra show equal altitude peaks because of the temperature difference between each enclosure side and the bundle of the three inner cylinder is uniform as shown in Fig.6 a, E=0.2. The peaks are increased at the upper sides with increasing Ra and vise versa at the bottom side due to the increase of free convection. A symmetry of the flow patterns is clearly proven by the symmetric local Nusselt number distributions, the sharp peaks are clearly due to impingement of the thermal plumes from the inner cylinders to the apex regions of the triangular enclosure.

The average Nusselt number is utilized to represent the overall heat transfer rate within the domain of interest. The overall average Nusselt number around both the inner surfaces and outer surface can be written as:

$$\overline{Nu_i} = \int_{s1} Nu_1.ds_1 + \int_{S_2} Nu_2.ds_2 + \int_{S_3} Nu_3.ds_3 \ , \ \overline{Nu_o} = \int_{S_0} Nu_o.ds_o \qquad (9)$$

At steady-state, it is obvious that the average Nusselt numbers along both the inner and outer cylinders are exactly identical. Hence, the average Nusselt number can be evaluated as:

$$\overline{Nu} = \overline{Nu_i} = \overline{Nu_o} \qquad (10)$$

This is plotted in Fig.8. The figure shows significant enhancement of the overall heat transfer by natural convection at constant E. However as E is further increased, the average Nusselt numbers are significantly increased. The most important advantage of the present work is illustrated in Fig.9, where for same surface area of single rod with D/H=1/2 [7] and D/H=1/6 of three rods, it is evidence that the average Nusselt number is significantly increased (about 65 % for E= 0.6 and about 20% for E=0.5). This increase in Nusselt number is attributed to the substantial contribution of the conduction heat transfer when the heated rods become closer to the enclosure walls.

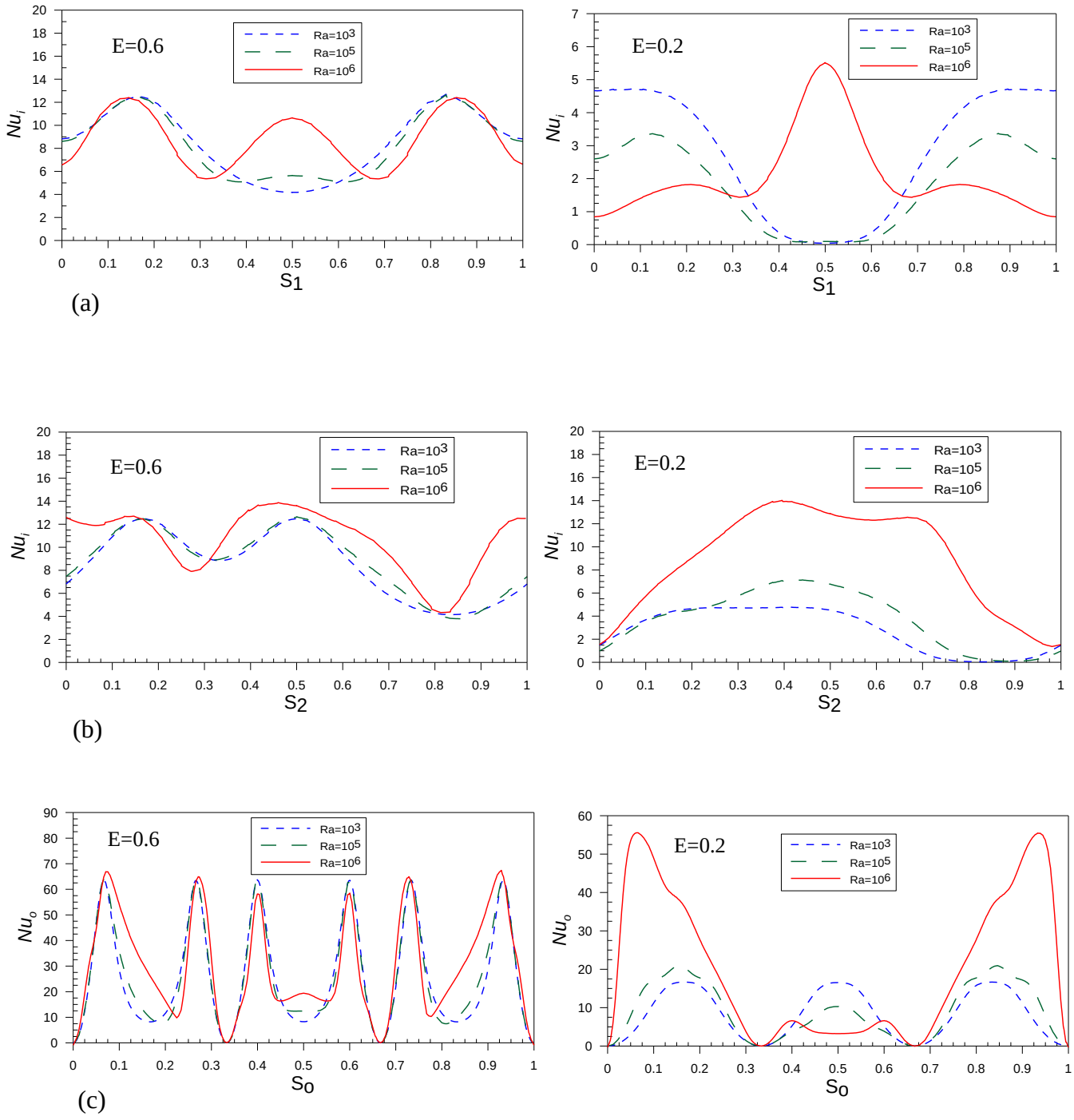


Fig. 7 Variation of the local Nusselt number on (a) upper rod, (b) left bottom rod and (c) triangle walls

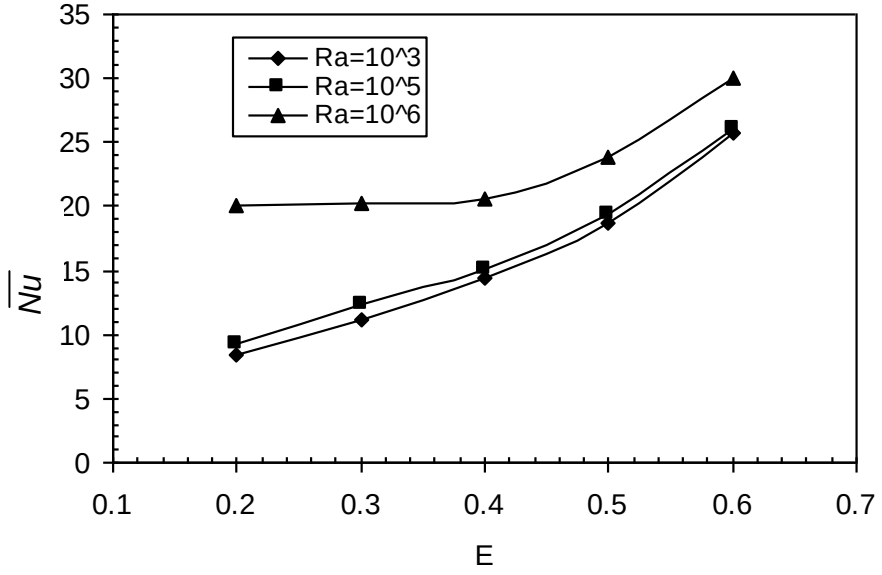


Fig.8 Variation of the average Nusselt number on the enclosure wall as a function of E for different Rayleigh numbers

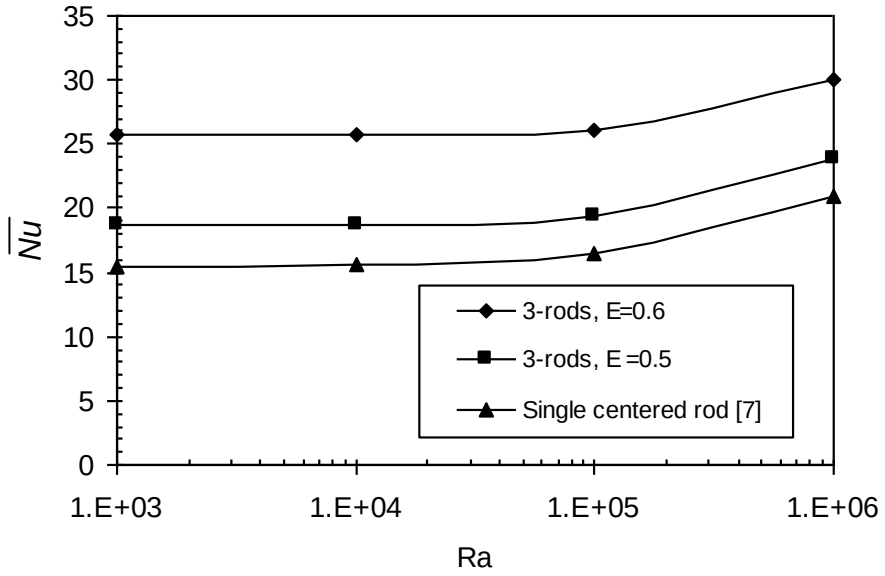


Fig. 9 Advantage of 3-rods, D/H=1/6 over single centered rods D/H=1/2

## 5. Conclusions

In the present paper, a numerical investigation of steady laminar natural convection in horizontal enclosure between equilateral triangle and inner heated rods was achieved. The effects of Rayleigh number and location of inner heated rods were systematically studied. The conclusions can be drawn as follows:

1- The average Nusselt number could be significantly increased by using more than one inner cylindrical rod even when the rods global surface area equals to that of single rod.

2- As Rayleigh number is increased, the streamlines and isotherms become less symmetric, and the formation of thermal plumes impinging to the top corner of the enclosure is noticed.

3- The overall heat transfer is significantly enhanced with increasing Rayleigh number due to more contribution from natural convection.

4- At large distance E, and with increasing Ra, the flow intensity and eddies are concentrated in the region between inner heated rods. At low E, the flow intensity becomes more concentrated around inner surfaces.

5- A symmetry of the flow patterns is occurred at larger distance E, and this symmetry clearly proven by symmetric local Nusselt number distributions. More peaks and troughs are observed for local Nusselt number distribution along inner surfaces.

## References

[1] Flack R.D., Konopnicki T.T. and Rooke, J.H. "The measurement of natural convective heat transfer in triangular enclosures" ASME J. Heat Transfer **101** 1979 pp648–654.

[2]Flack R.D. "The experimental measurement of natural convection heat transfer in triangular enclosures heated or cooled from below", ASME J. Heat Transfer **102** 1980 pp 770–772.

[3] Uzun Ibrahim and Usnal Mazhar " A numerical study of laminar heat concevtion in ducts of irregular cross-sections" Int. Comm. Heat Mass Transfer vol.24 No. 6 1997 pp 835-848

[4] Asan, H. and Namli L. "Laminar natural convection in a pitched roof of triangular cross-section: summer day boundary conditions" Energy and Buildings **33** 2000 pp 69-73

[5] E. Fuad Kent "Numerical analysis of laminar natural convection in isosceles triangular enclosures for cold base and hot inclined walls" Mechanics Research Communications **36** 2009 pp 497–508

[6] Venkateswara Roa M, Ravi Kumar P.V. and Sankara Rao P.S. "Laminar flow heat transfer in concentric equilateral triangular annular channel" Indian Journal of Chemical Technology vol. 13, 2006 pp. 614-622

[7] X Xu , Yu Z., Hu Y, Fan L. and Cen K. " A numerical study of laminar natural convective heat transfer around a horizontal cylinder inside a concentric air-filled triangular enclosure" International Journal of Heat and Mass Transfer **53** 2010 pp 345–355

[8] Backstrom Gunnar "Fields of Physics by Finite Element Analysis Using FlexPDE" by GB Publishing and Gunnar Backstrom Malmo, Sweden 2005

[9] Langtangen H. P., Mardal K.A. and Winther R. " Numerical methods for incompressible viscous flow" Advances in Water Resources **25** 2002 pp 1125–1146

[10] Moukalled F. and Acharya S. "Natural convection in the annulus between concentric horizontal circular and square cylinders", AIAA J. Thermophys. Heat Transfer **10** 1996 pp 524–531

## Nomenclature

| | | | |
|---|---|---|---|
| D | rod diameter (m) | u, U | horizontal velocity, dimensional (m/s) and dimensionless |
| e,E | distance between inner rods center and enclosure center, dimensional (m) and dimensionless | v, V | vertical velocity, dimensional (m/s) and dimensionless |
| h | heat transfer coefficient ($W/m^2 K$) | *Greek symbols* | |
| H | enclosure height (m) | α | thermal diffusivity ($m^2/s$) |
| k | thermal conductivity of fluid (W/m K) | β | thermal expansion coefficient (1/K) |
| L | enclosure side length (m) | λ | Penalty parameter ( $N/m^4.s$) |
| Nu | local Nusselt number | υ | kinematic viscosity ($m^2/s$) |
| $\overline{Nu}$ | Average Nusselt number | μ | Dynamic viscosity ($N/m^2.s$) |
| p, P | pressure, dimensional (Pa) and dimensionless | ρ | fluid density ($kg/m^3$) |
| Pr | Prandtl number | θ | dimensionless temperature |
| Ra | Rayleigh number | *Subscripts* | |
| S | local coordinate, dimensionless. | i | inner |
| T | temperature (K) | o | outer |